

## Elastic and inelastic scattering of 0.8 GeV polarized protons from $^{24}\text{Mg}$ and $^{26}\text{Mg}$

G. S. Blanpied and B. G. Ritchie\*

*University of South Carolina, Columbia, South Carolina 29208*

M. L. Barlett, G. W. Hoffmann, J. A. McGill,<sup>†</sup> and E. C. Milner<sup>†</sup>

*University of Texas, Austin, Texas 78712*

K. W. Jones<sup>†</sup> and S. K. Nanda<sup>‡</sup>

*Rutgers University, New Brunswick, New Jersey 08903*

R. de Swiniarski<sup>§</sup>

*Rutgers University, New Brunswick, New Jersey 08903*

*and Institut des Sciences Nucléaires, Grenoble, France*

(Received 28 September 1987)

Data on 800 MeV polarized proton scattering on  $^{24}\text{Mg}$  and  $^{26}\text{Mg}$  are presented. Angular distributions and analyzing power data have been extracted from fits to 26 peaks in the spectra for  $^{24}\text{Mg}$  and 23 peaks in  $^{26}\text{Mg}$ . Although there are a variety of shapes for the angular distributions, the analyzing power data for all states are positive and similar in magnitude and seem to be consistent with a two-body operator for the excitation with a spin structure much like that for the free proton-nucleon system. Evidence for a level in  $^{26}\text{Mg}$  at 8.03 MeV with  $J > 4$  is presented. Comparison between the observed angular distribution, coupled channels, and distorted wave Born approximation calculations, and the angular distributions of excited states in neighboring nuclei, support the assignment of  $J^\pi = 5^-$  or  $6^+$ . Coupled channels calculations for the  $0^+$ ,  $2^+$ ,  $4^+$ , and  $6^+$  members of the ground state rotational bands of  $^{24}\text{Mg}$  and  $^{26}\text{Mg}$  are compared to the data. Deformation parameters from distorted wave Born approximation calculations are determined for most of the angular distributions.

### I. INTRODUCTION

Rotational band structure has been recognized as a systematic feature in the spectra of light nuclei with  $20 < A < 28$ , thus with partially filled  $s$ - $d$  shell levels. In addition to the resemblance of the observed series of levels to established features of collective bands, such proposals have been supported quite well by collective model coupled channels calculations (CC) in several cases.<sup>1-7</sup> These calculations reproduce most of the measured angular distributions of proton excitation of these levels, giving strong support for the assignment of these levels to collective rotational bands.

A good example<sup>1</sup> is  $^{24}\text{Mg}$ : The states in  $^{24}\text{Mg}$  can be grouped into a ground state rotational band (GSRB) consisting of the (0.0 MeV,  $0^+$ ), (1.37,  $2^+$ ), (4.12,  $4^+$ ), and (8.12,  $6^+$ ) levels. Additionally there is evidence for  $K^\pi = 2^+$ ,  $0^+$ ,  $0^-$ , and  $3^-$  bands. In fact, nearly all levels below 10 MeV in  $^{24}\text{Mg}$  are believed to belong to rotational bands. Aside from  $^{24}\text{Mg}$ , levels in  $^{20}\text{Ne}$ ,  $^{22}\text{Ne}$ , and  $^{28}\text{Si}$  have been assigned to a GSRB, and the  $6^+$  member of the GSRB's in each of these nuclei has been observed.<sup>8</sup> The extension of these ideas to  $^{26}\text{Mg}$  would seem to be straightforward. However, no natural parity level in  $^{26}\text{Mg}$  with spin greater than 4 has been reported. The collective description of  $^{26}\text{Mg}$  has been based upon a series of limited bands, with some evidence of band mixing.<sup>1,4,6,7</sup> The recent report of  $8^+$  and  $10^+$  levels of the  $^{28}\text{Si}$  GSRB (Ref. 9) has further supported a collective

description of this nucleus, and has stimulated efforts to find high spin levels in  $^{26}\text{Mg}$ .

In a previous analysis<sup>1</sup> of unpolarized proton angular distributions from  $^{24}\text{Mg}$  and  $^{26}\text{Mg}$  CC analyses of the two GSRB, possible  $\gamma$ -vibrational bands ( $K^\pi = 2^+$ ), and octupole vibrational bands ( $K^\pi = 0^-$  and  $3^-$ ) were able to explain the magnitude and shape of the angular distributions. The multipole moments of the deformed optical potential used in the calculations were generally  $\sim 10\%$  lower in the case of  $^{24}\text{Mg}$  and  $\sim 25\%$  lower in the case of  $^{26}\text{Mg}$ , than those from low energy hadronic measurements and electromagnetic measurements.

In order to search for high spin states in  $^{26}\text{Mg}$ , to investigate possible spin dependent effects, and to specify spin-orbit potential parameters, we have made measurements on the scattering of 0.8 GeV polarized protons from  $^{24}\text{Mg}$  and  $^{26}\text{Mg}$ . Angular distributions and analyzing power data for peaks up to an excitation energy of 15.5 MeV in  $^{24}\text{Mg}$  and 10.4 MeV in  $^{26}\text{Mg}$  have been obtained. Data for 26 excited peaks in  $^{24}\text{Mg}$  and 23 peaks in  $^{26}\text{Mg}$  are reported here. Because of the level spacing in these isotopes and the experimental resolution, most of these peaks consist of one, or one dominant, excited state. A CC analysis of the data for both isotopes, including a proposed  $6^+$  for  $^{26}\text{Mg}$ , is presented here. A single step distorted wave Born approximation (DWBA) analysis of the other states has been performed in order to identify, if possible, the angular momentum transfer and remaining multistep effects.

## II. EXPERIMENT

The experiment was performed using the High Resolution Spectrometer (HRS) at the Clinton P. Anderson Meson Physics Facility of the Los Alamos National Laboratory. Details of the beam line, spectrometer, focal plane instrumentation, and beam polarization monitors have been reported elsewhere.<sup>10</sup> The beam polarization was stable and greater than 0.8. Targets enriched to more than 99% of  $^{24}\text{Mg}$  (19.6 mg/cm<sup>2</sup>) and  $^{26}\text{Mg}$  (26.3 mg/cm<sup>2</sup>) were used, and an energy resolution of  $\sim 80$  keV was obtained. This resolution allowed the extraction of peak areas up to an energy of 15.5 MeV in  $^{24}\text{Mg}$  and to 10.4 MeV in  $^{26}\text{Mg}$ . Differential cross sections and analyzing powers were measured from  $5^\circ$  to  $25.4^\circ$  cm with angular resolution of  $0.1^\circ$ . The data are presented in Figs. 1–29. Tabulated results are deposited in PAPS.<sup>11</sup>

## III. GROUND STATE ROTATIONAL BANDS

### A. Coupled channels calculations

CC calculations of the cross section and analyzing power data for the  $0^+$ ,  $2^+$ ,  $4^+$ , and  $6^+$  states of the GSRB of  $^{24}\text{Mg}$  and  $^{26}\text{Mg}$  have been performed. These calculations are similar to those reported in Ref. 1. Since the code JUPITER used in Ref. 1 does not include the deformed spin-orbit potential to all orders, the code ECIS (Ref. 12) has been used here. The angular distribution  $\sigma(\theta)$  and analyzing power ( $A_y$ ) data given in Figs. 1–4 are included in a chi-squared search of a deformed poten-

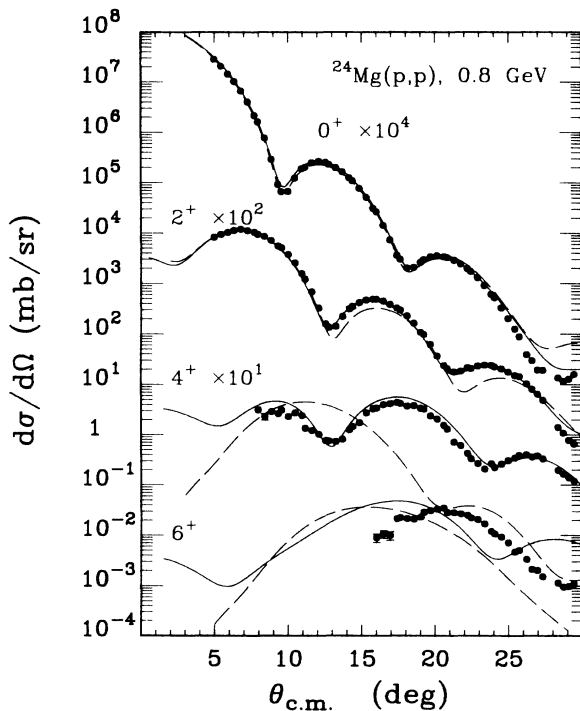


FIG. 1. Angular distributions for the  $0^+$ ,  $2^+$ ,  $4^+$ , and  $6^+$  states in  $^{24}\text{Mg}$ , multiplied by  $10^4$ ,  $10^2$ , 10, and 1, respectively, along with the results from coupled channels (solid lines) and DWBA (dashed lines) calculations as discussed in the text.

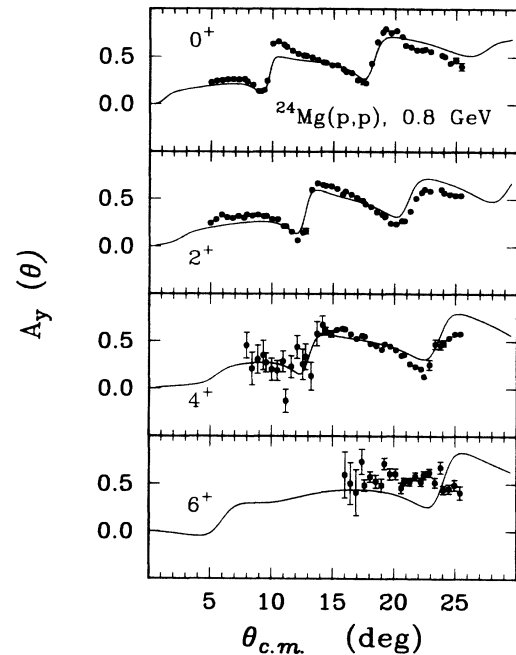


FIG. 2. Analyzing powers for the  $0^+$ ,  $2^+$ ,  $4^+$ , and  $6^+$  states in  $^{24}\text{Mg}$  along with results from coupled channels calculations as discussed in the text.

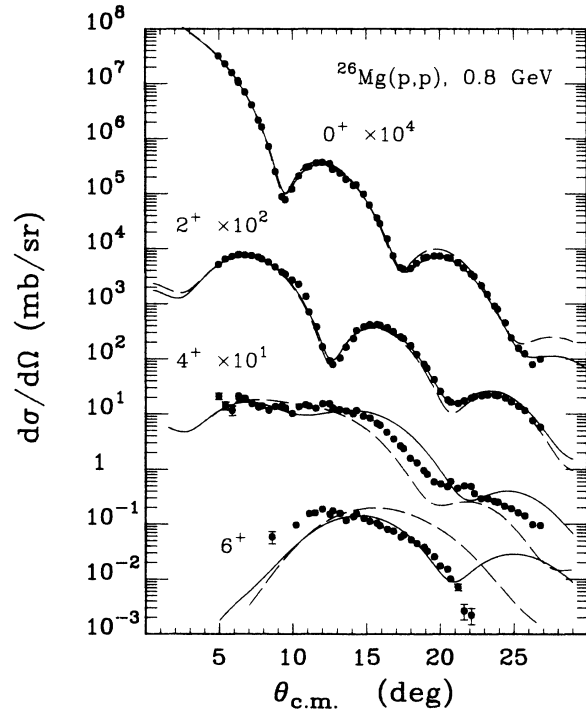


FIG. 3. Angular distributions for the  $0^+$ ,  $2^+$ ,  $4^+$ , and proposed  $6^+$  states in  $^{26}\text{Mg}$  multiplied by  $10^4$ ,  $10^2$ , 10, and 1, respectively, along with results from coupled channels (solid lines) and DWBA (dashed lines) calculations. A DWBA calculation for an unresolved  $2^+$  has been added incoherently to the predictions for the  $4^+$  state.

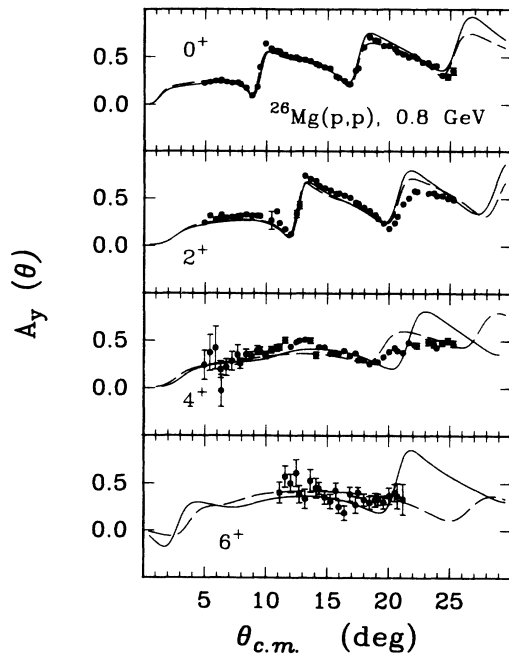


FIG. 4. Analyzing powers for the  $0^+$ ,  $2^+$ ,  $4^+$ , and proposed  $6^+$  states in  $^{26}\text{Mg}$  along with results from coupled channels (solid lines) and DWBA (dashed lines) calculations. The proper summation has been made for the unresolved  $2^+ + 4^+$  states, using a DWBA calculation for the  $2^+$  state.

tial including the real and imaginary spin-orbit terms. The parameters for the potentials and densities are given in Table I, and the results are shown as solid lines in the figures. DWBA calculations using a spherically symmetric ground state potential are shown as dashed lines in the figures; the potential parameters are also given in Table I. The cross section and analyzing powers for  $0^+$ ,  $2^+$ , and  $4^+$  states of  $^{24}\text{Mg}$  and the  $0^+$  and  $2^+$  states of  $^{26}\text{Mg}$  are well explained by the CC calculations. The extreme backward peaking of the angular distribution for the  $6^+$  in  $^{24}\text{Mg}$  probably results from the difference in in-

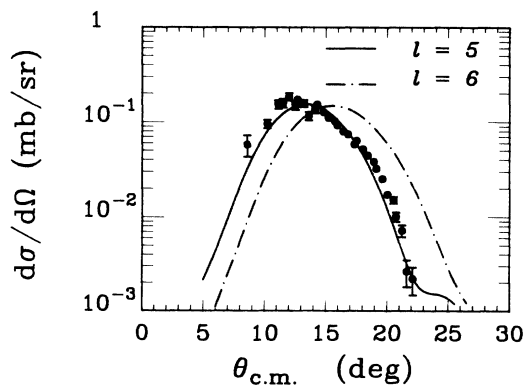


FIG. 5. Comparison of the measured angular distribution for the 8.03 MeV level in  $^{26}\text{Mg}$  with DWBA calculations, assuming  $l=5$  (solid line,  $\beta_5=0.042$ ) and  $l=6$  (dashed lines,  $\beta_6=0.048$ ).

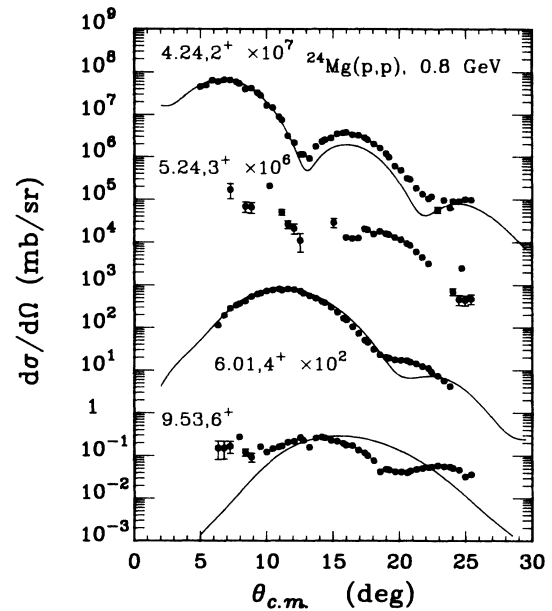


FIG. 6. Angular distributions and DWBA calculations for 4.24, 5.24, 6.01, and 9.53 MeV states in  $^{24}\text{Mg}$ . The deformation parameters are given in Table II and the values for the potential in Table I.

terference between the direct step and multistep excitation of this level. The fit could perhaps be improved by allowing the  $l=2$  coupling between the  $2^+$  and  $4^+$  and between the  $4^+$  and  $6^+$  to vary from the rigid rotor values. The rather flat prediction of  $A_y$  for the  $6^+$  is lower than the fairly constant experimental value.

As seen in Figs. 3 and 4, both CC and DWBA calcula-

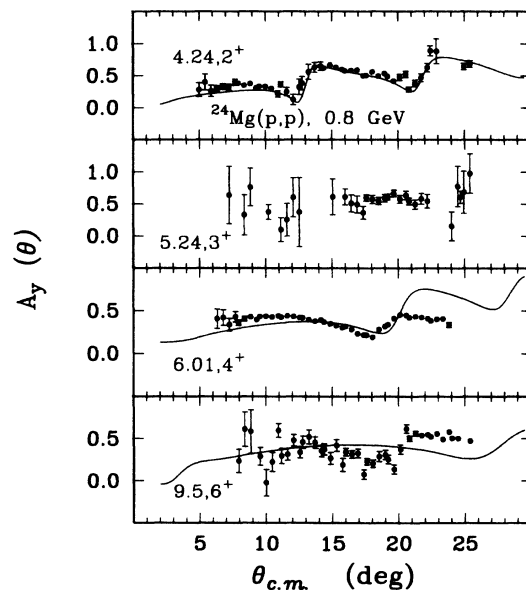


FIG. 7. Analyzing powers and DWBA calculations for the 4.24, 5.24, 6.01, and 9.53 MeV states in  $^{24}\text{Mg}$ .

TABLE I. Potential parameters for coupled channels and DWBA analyses described in the text. One geometry is used for the real and imaginary volume potentials and another for the real and imaginary spin-orbit terms.

	Coupled channels		DWBA	
	$^{24}\text{Mg}$	$^{26}\text{Mg}$	$^{24}\text{Mg}$	$^{26}\text{Mg}$
$V$ (MeV)	-3.8	-4.6	-1.5	-3.2
$W$ (MeV)	94.0	67.4	83.5	64.0
$r$ (fm)	0.910	0.990	0.914	1.021
$a$ (fm)	0.590	0.563	0.660	0.574
$V_{s0}$ (MeV)	0.951	0.715	0.950	0.910
$W_{s0}$ (MeV)	2.26	2.24	2.02	2.49
$r_{s0}$ (fm)	0.910	0.983	0.914	0.953
$a_{s0}$ (fm)	0.590	0.552	0.660	0.637
$\beta_2$	0.592	0.448		
$\beta_4$	-0.022	-0.105		
$\beta_6$	-0.016	-0.020		

tions are able to explain the cross section and analyzing power data for the  $0^+$  and  $2^+$  states in  $^{26}\text{Mg}$ . The data for the  $4^+$  are actually that for an unresolved doublet ( $2^+ + 4^+$ ). Since the  $2^+$  and  $4^+$  angular distributions are out of phase until about  $17^\circ$  and are of comparable magnitude, the observed  $\sigma(\theta)$  is flat until about  $15^\circ$ . The first minimum of  $2^+$  states for this nucleus are in the region of the first maximum for  $4^+$  states, and it is the data around  $12^\circ \pm 2^\circ$  that is indicative of the  $4^+$  strength. An incoherent sum of cross sections of a DWBA calculation for the  $2^+$  with  $\beta_2=0.064$  with the CC result for the  $4^+$  is given by the solid line in Figs. 3 and 4. The dashed lines result from incoherent sums of the DWBA calculations for both of these states with  $\beta_2=0.064$  and

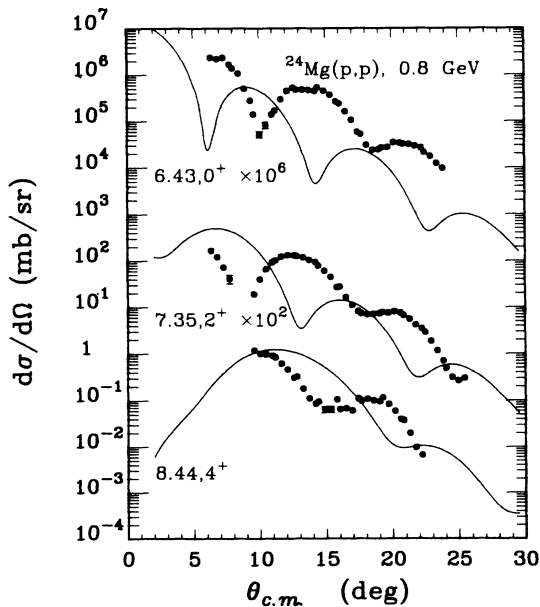


FIG. 8. Same as Fig. 6 for the 6.43, 7.35, and 8.44 MeV states in  $^{24}\text{Mg}$ .

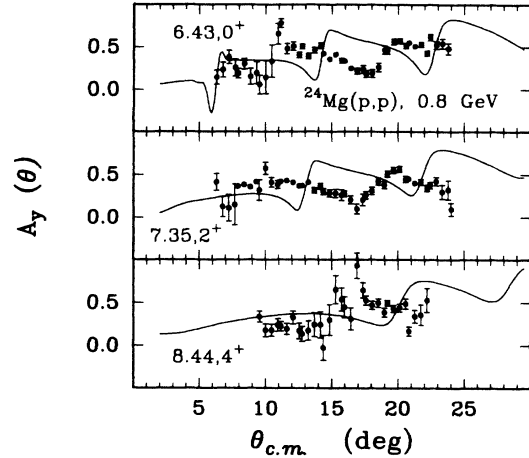


FIG. 9. Same as Fig. 7 for the 6.43, 7.35, and 8.44 MeV states in  $^{24}\text{Mg}$ .

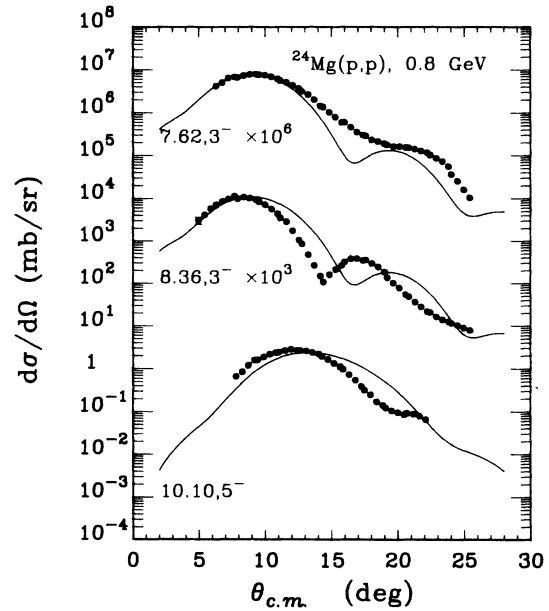


FIG. 10. Same as Fig. 6 for the 7.62, 8.36, and 10.10 MeV states in  $^{24}\text{Mg}$ .

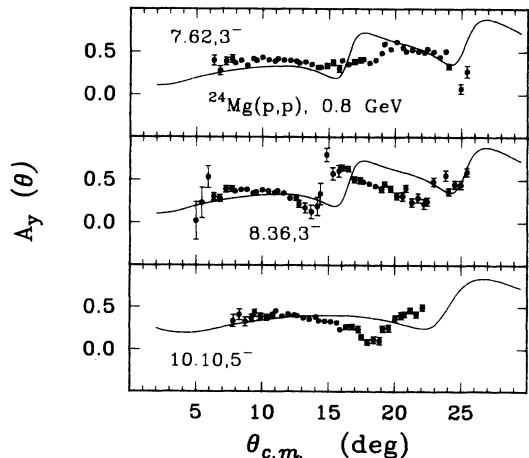


FIG. 11. Same as Fig. 7 for the 7.62, 8.36, and 10.10 MeV states in  $^{24}\text{Mg}$ .

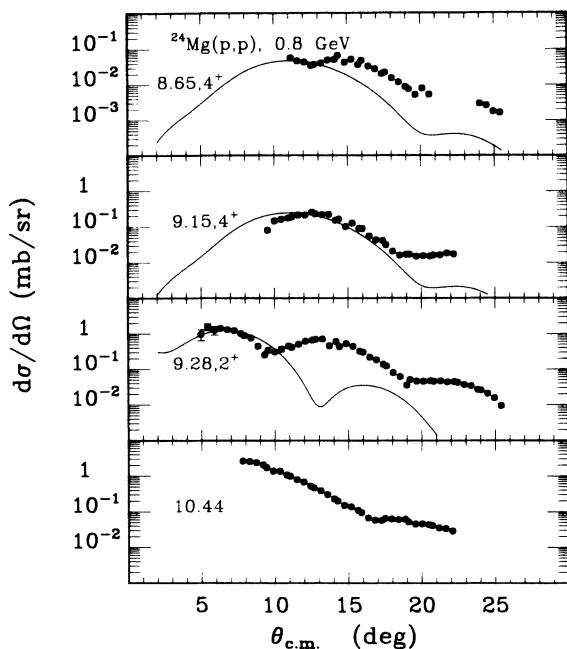


FIG. 12. Same as Fig. 6 for the 8.65, 9.15, 9.28, and 10.44 MeV states in  $^{24}\text{Mg}$ .

$\beta_4=0.100$ . The resulting fits to the data are good in magnitude but the point where the cross section falls off is difficult to reproduce, falling between the DWBA and CC results. An additional shortcoming arises in reproducing the magnitude of  $A_y$  in the region of the maximum  $4^+$  cross section. Some authors have included both the  $4_1^+$  and  $4_2^+$  states as mixed members of the GSRB.<sup>6,7</sup>

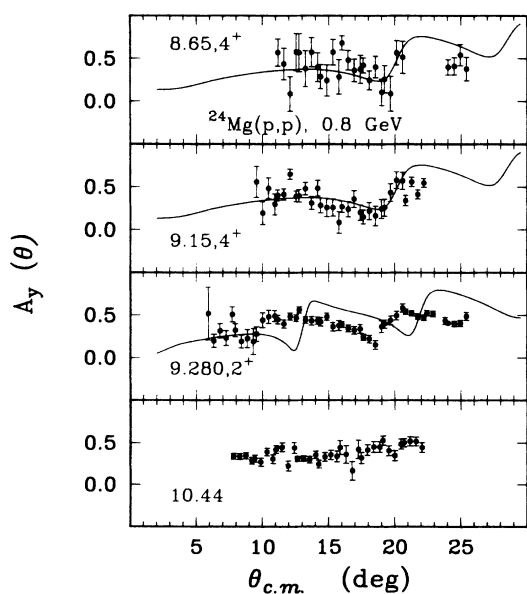


FIG. 13. Same as Fig. 7 for the 8.65, 9.15, 9.28, and 10.44 MeV states in  $^{24}\text{Mg}$ .

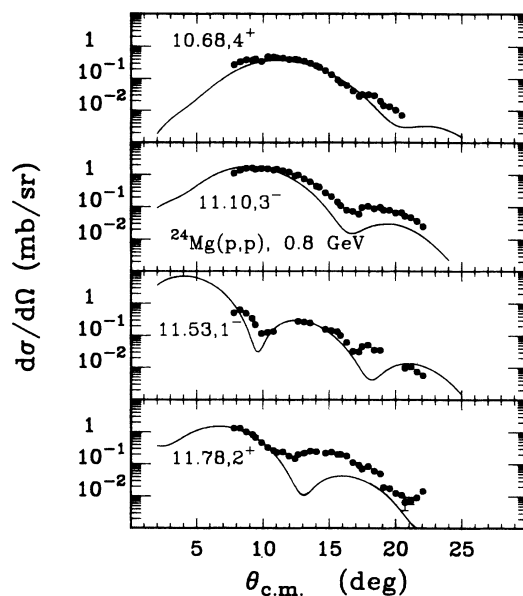


FIG. 14. Same as Fig. 6 for the 10.68, 11.10, 11.53, and 11.78 MeV states in  $^{24}\text{Mg}$ .

#### B. Evidence for a $6^+$ level in a GSRB

The level at 8.03 MeV in  $^{26}\text{Mg}$  has been assumed to be the  $6^+$  member of the ground state band. The evidence for this level to be a  $6^+$  is largely circumstantial and a definitive assignment cannot be made. The following observations yield support to a  $5^-$  or  $6^+$  assignment for this

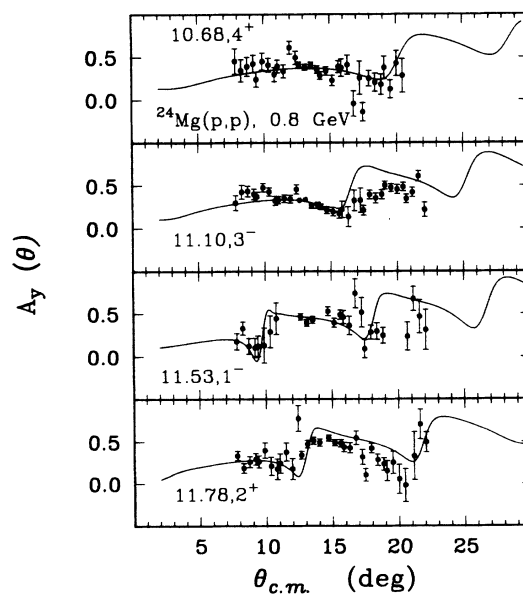


FIG. 15. Same as Fig. 7 for the 10.68, 11.10, 11.53, and 11.78 MeV states in  $^{24}\text{Mg}$ .

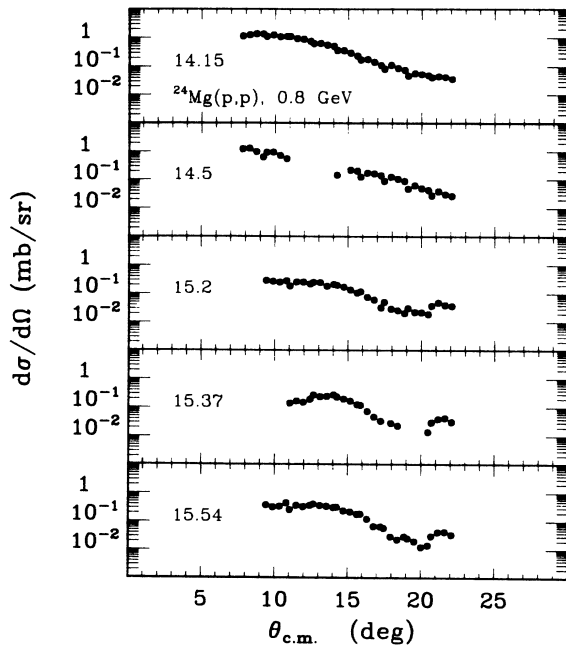


FIG. 16. Angular distributions for the 14.15, 14.50, 15.20, 15.37, and 15.54 MeV states in  $^{24}\text{Mg}$ . The state labeled 15.2 MeV may be the (15.137,  $6^-$ ,  $T=1$ ) state (Ref. 17).

level.

(1) *The position of the first maximum in the angular distribution with respect to other states of known spin in  $^{26}\text{Mg}$  implies a transferred angular momentum greater than 4, indicating the excitation of a state with  $J > 4$ . While the distribution seen in Fig. 3 peaks at about  $13^\circ$ , the  $4^+$  levels peak at approximately  $11^\circ$ , with all other*

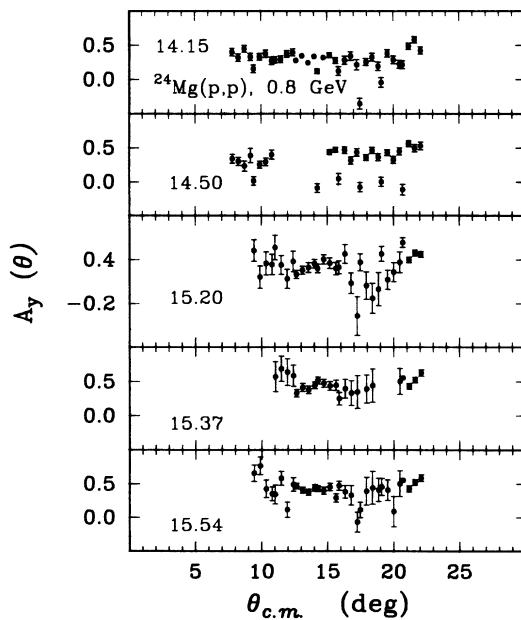


FIG. 17. Analyzing powers for the 14.15, 14.50, 15.20, 15.37, and 15.54 MeV states in  $^{24}\text{Mg}$ .

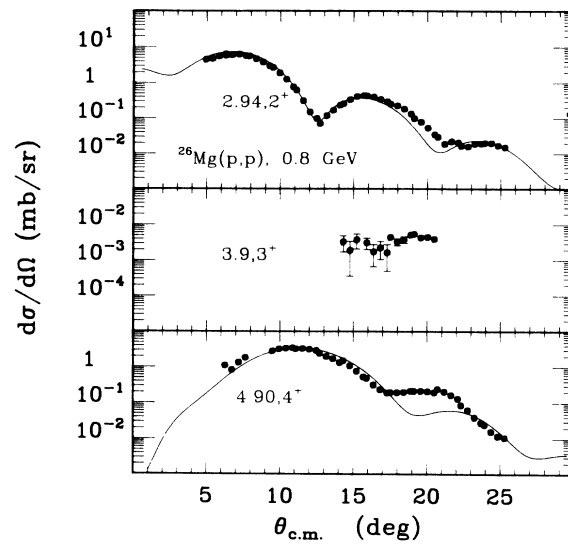


FIG. 18. Angular distributions and DWBA calculations for the 2.94, 3.94, and 4.90 MeV states in  $^{26}\text{Mg}$ . The deformation parameters and parameters for the potential are given in Tables I and III.

levels of known spin peaking at smaller angles.

(2) *The magnitude of the cross section is most likely too large for an unnatural parity state, since the spin-flip probability is small at 800 MeV.*

(3) *The CC calculation for a  $6^+$  level in a GSRB reproduces reasonably well the observed angular distribution, though perfect agreement is not achieved. The value of  $\beta_6$  is small ( $-0.02$ ) so that multistep effects are large. The magnitude of the differential cross section is well pre-*

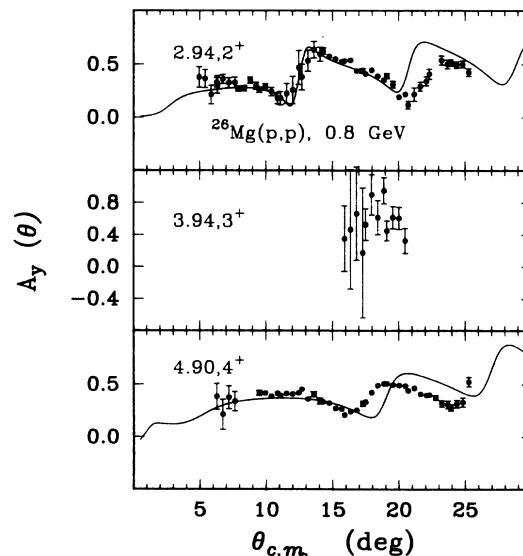


FIG. 19. Analyzing powers and DWBA calculations for the 2.94, 3.94, and 4.90 MeV states in  $^{26}\text{Mg}$ .

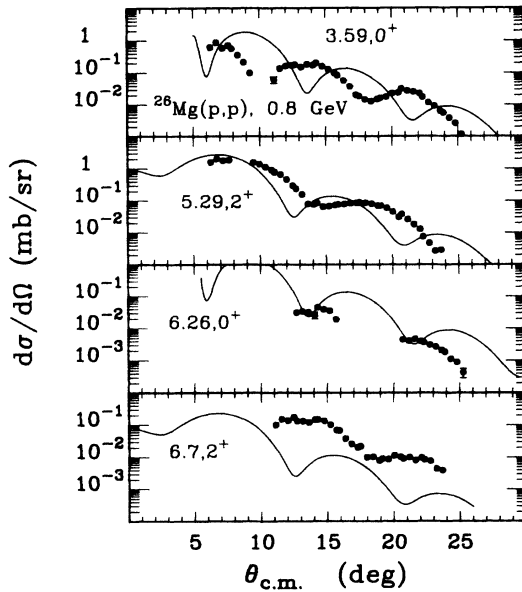


FIG. 20. Same as Fig. 18 for the 3.59, 5.29, 6.26, and 6.74 MeV states in  $^{26}\text{Mg}$ .

dicted except at the most backward angles, where other channels of the reaction process may contribute. The present codes do not include a  $Y_{50}$  term in the Hamiltonian, thus preventing coupled channel calculations assuming a  $5^-$  level. In the  $K^\pi=0^-$  ( $1^-, 3^-, 5^-$ ) band of  $^{24}\text{Mg}$ , it was noted that coupled channels calculations for the  $5^-$  level which did not include such a direct step from the ground state were an order of magnitude too low in predicting the observed angular distribution.<sup>3</sup>

(4) DWBA calculations for an  $l=5$  angular distribution

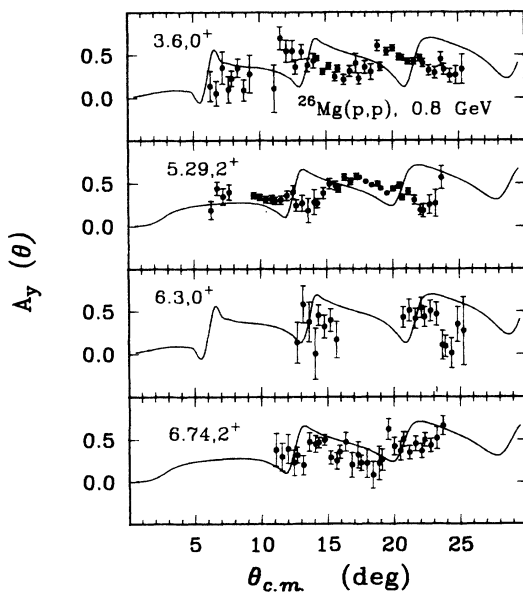


FIG. 21. Same as Fig. 19 for the 3.59, 5.29, 6.26, and 6.74 MeV states in  $^{26}\text{Mg}$ .

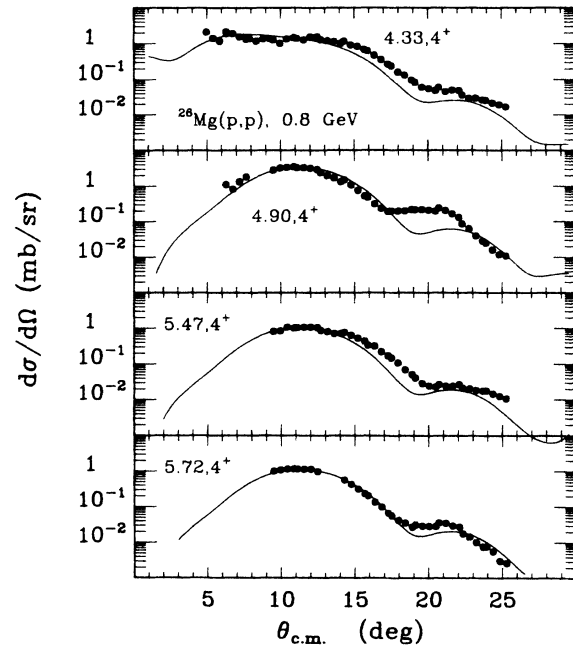


FIG. 22. Same as Fig. 18 for states excited by  $l=4$ , the 4.33 (with incoherent admixture of  $2^+$ ), 4.90, 5.47, and 5.72 MeV states in  $^{26}\text{Mg}$ .

reproduce the observed phenomena quite well. The results of these calculations shown in Fig. 5, where the potential used is that given in Table I. Here values of  $\beta_5=0.042$  and  $\beta_6=0.048$  are used. A general feature of high spin DWBA calculations performed on nuclei in this region is that the angular distributions predicted by the calculations peak at larger angles than observed. Hence

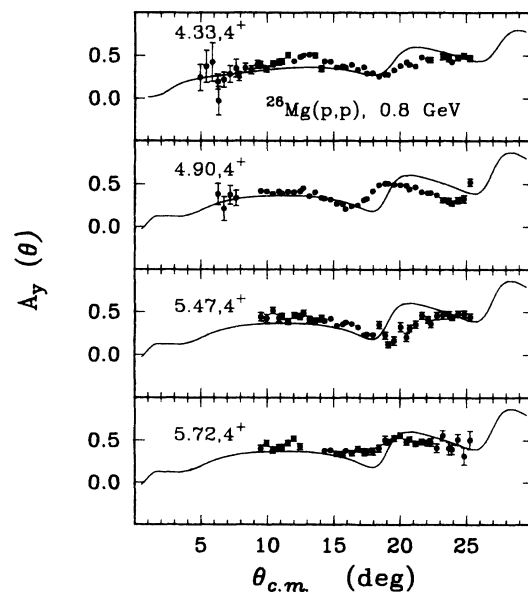


FIG. 23. Same as Fig. 19 for the 4.33 (with incoherent admixture of  $2^+$ ), 4.90, 5.47, and 5.72 MeV states in  $^{26}\text{Mg}$ .

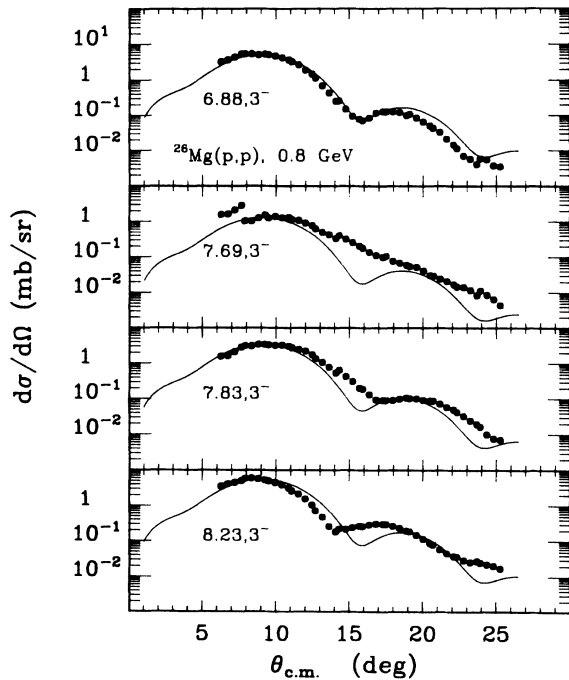


FIG. 24. Same as Fig. 18 for states excited by  $l=3$ , the 6.88, 7.69, 7.83, and 8.23 MeV states in  $^{26}\text{Mg}$ .

these calculations support an assignment of  $J > 5$  since, as seen in the figure, the  $l=5$  distribution matches the peak quite well, while the  $l=6$  curve is seen to peak at a larger angle than measured. Though the validity of applying DWBA calculations to deformed nuclei is questionable, it is interesting to note that a satisfactory fit to the data

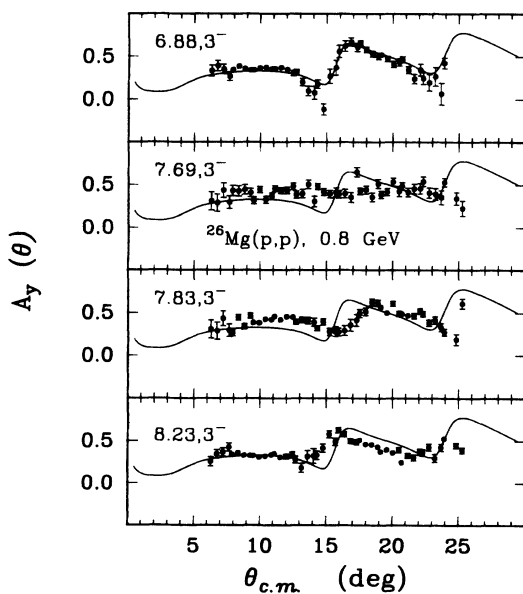


FIG. 25. Same as Fig. 19 for the 6.88, 7.69, 7.83, and 8.23 MeV states in  $^{26}\text{Mg}$ .

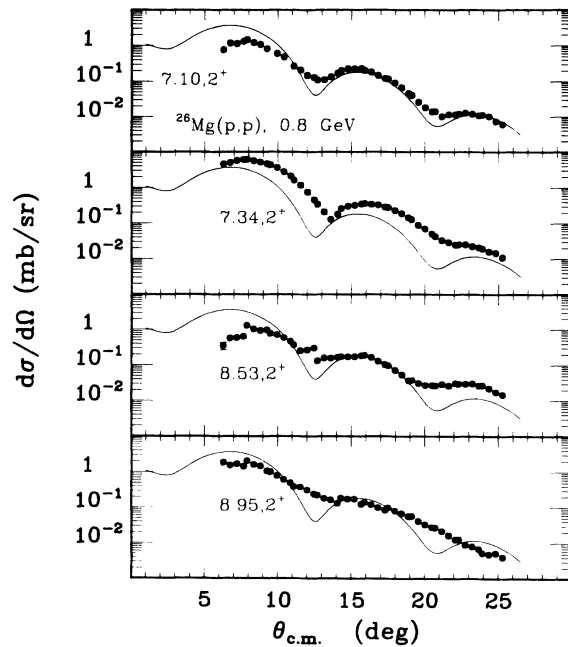


FIG. 26. Same as Fig. 18 with  $l=2$  DWBA predictions for the 7.10, 7.34, 8.53, and 8.95 MeV states in  $^{26}\text{Mg}$ .

may be obtained by such a spherical potential and no coupling.

(5) *Comparison with known  $6^+$  levels in  $^{24}\text{Mg}$*  can suggest by arguments based on systematics that the level at 8.03 MeV may be a  $6^+$  state. Cross section data for the first two  $6^+$  and the  $5^-$  states in  $^{24}\text{Mg}$  are shown in Figs. 1, 6, and 10. The  $6_1^+$  level of  $^{24}\text{Mg}$  is observed at 8.12 MeV, which is very nearly the same in energy as the 8.03

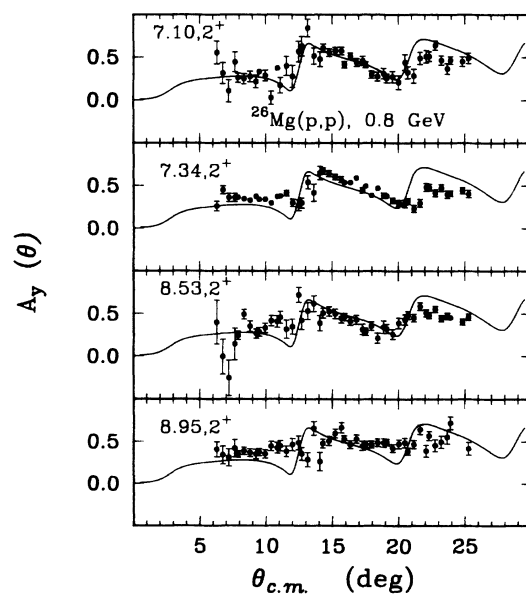


FIG. 27. Same as Fig. 19 for the 7.10, 7.34, 8.53, and 8.95 MeV states in  $^{26}\text{Mg}$ .



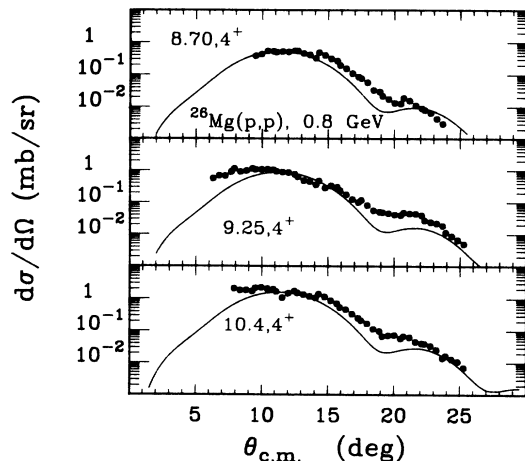


FIG. 28. Same as Fig. 18 with  $l=4$  DWBA predictions for the 8.70, 9.25, and 10.40 MeV states in  $^{26}\text{Mg}$ .

MeV observed for the level under discussion, though the angular distributions are not similar. However, another level at 9.53 MeV in  $^{24}\text{Mg}$  has been identified as the  $6_2^+$  level, and its shape (peaking at about  $14^\circ$ ) and its magnitude at maximum ( $\sim 0.3$  mb) bear a strong resemblance to the 8.03 MeV level in  $^{26}\text{Mg}$ . The DWBA calculation shown in Fig. 6 for the  $6_2^+$  state is observed to peak at a greater angle than the data. The lack of resemblance between the 8.12 MeV level in  $^{24}\text{Mg}$  and the 8.03 MeV level in  $^{26}\text{Mg}$  probably results from the difference in interference between the direct step and multistep excitation for those levels. It is this interference which results in an angular distribution for the  $^{24}\text{Mg}$   $6_1^+$  level which peaks at an angle of  $20^\circ$  as compared to an expected value of about  $13^\circ$ .

The angular distribution for the ( $5^-$ , 10.03 MeV) level in  $^{24}\text{Mg}$  given in Fig. 10 is observed to peak at  $12^\circ$ , while the DWBA calculation peaks at about  $13.5^\circ$ . Additionally, the magnitude of the cross section for the ( $5^-$ , 10.03

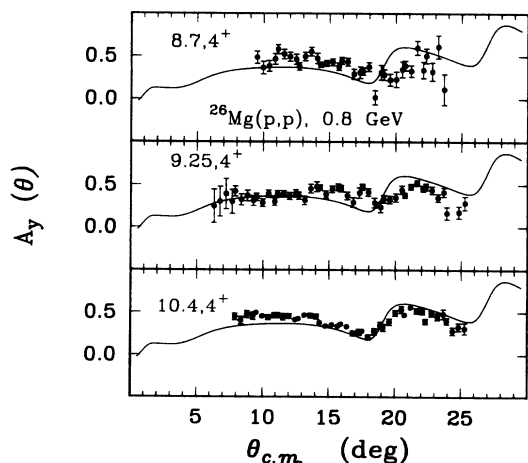


FIG. 29. Same as Fig. 19 for the 8.70, 9.25, and 10.40 MeV states in  $^{26}\text{Mg}$ .

TABLE II. Excitation energy (in MeV) of the first  $6^+$  states in several deformed  $s$ - $d$  shell nuclei. Rotor calculations based on  $4^+ \rightarrow 2^+$  transition energy. CW denotes shell model calculations using Chung-Wildenthal interaction (Ref. 13).

	$^{20}\text{Ne}$	$^{22}\text{Ne}$	$^{24}\text{Mg}$	$^{28}\text{Si}$	$^{26}\text{Mg}$
Observed	8.78	6.31	8.11	8.54	(8.03) <sup>a</sup>
Rotor	8.36	6.63	8.45	9.08	8.29
CW	8.54	6.26	8.47	9.06	8.73

<sup>a</sup>Proposed here as  $6^+$ .

MeV) level in  $^{24}\text{Mg}$  is more than an order of magnitude greater at its peak than the 8.03 MeV level in  $^{26}\text{Mg}$ . Thus, the systematics of the angular distributions for these states in  $^{24}\text{Mg}$  suggest that the 8.03 level in  $^{26}\text{Mg}$  is most probably a  $6^+$  state.

(6) *Agreement with rotor and shell model predictions* of energy of excitation also suggest that the observed level at 8.03 MeV may be a  $6^+$  level. Comparison with rigid rotor calculations for neighboring nuclei suggests that such a model may be a useful tool in predicting GSRB energies, though the energies predicted are usually higher than those observed, as shown in Table II. Basing the moment of inertia for  $^{26}\text{Mg}$  on the  $4^+ \rightarrow 2^+$  energy difference yields a prediction of 8.29 MeV for a GSRB  $6^+$  in  $^{26}\text{Mg}$  adding support to the assignment of  $l=6$  for the excitation of the 8.03 MeV level. Shell model calculations,<sup>13</sup> which are also given in Table II, again usually predict higher energies for the members of the GSRB than are observed (except for  $^{20}\text{Ne}$ ).

### C. Multipole moments

The problems with the fit to the  $6^+$  state in  $^{24}\text{Mg}$  and the correct choice for the  $6^+$  state in  $^{26}\text{Mg}$  have no effect on the parameters for the ground state and  $2^+$  and around 20% or less on the parameters for the  $4^+$  state if the values of  $\beta_6$  are not much larger than those employed here. The resulting moments for  $^{26}\text{Mg}$  as defined in Ref. 1 are  $M(E2) = +0.152 eb$ ,  $M(E4) = -0.0025 eb^2$ , and  $M(E6) = -0.0010 eb^3$ . Optical model uncertainties of  $\pm 0.01$  fm in “ $r$ ” and “ $a$ ” and  $\pm 0.02$  in  $\beta_2$ ,  $\beta_4$ , and  $\beta_6$  result in uncertainties in these moments of  $\pm 0.008$ ,  $\pm 0.0017$ , and  $\pm 0.0005$ , respectively. An uncertainty of  $\pm 0.02$  in  $\beta_6$  alone contributes  $\pm 0.0005$  in  $M(E2)$ ,  $\pm 0.0005$  in  $M(E4)$ , and  $\pm 0.0004$  in  $M(E6)$ . Thus knowledge of the  $6^+$  strength if indeed correct reduces the errors in  $M(E4)$  and  $M(E6)$  to the point where they are determined to be negative.

The  $M(E2)$  value for  $^{26}\text{Mg}$  is slightly higher than the value obtained in Ref. 1, which included no spin-orbit contribution and in which the potential was varied to fit the data “by hand,” not in an automated chi-square fashion as in the present analysis. This new value of  $M(E2)$ , combined with the new charge moment for  $^{26}\text{Mg}$  (Ref. 14) implies that the  $M(E2)$  moments of the neutron and proton distributions in  $^{26}\text{Mg}$  are approximately equal and prolate.

The values obtained for  $^{24}\text{Mg}$  are  $M(E2) = +0.187 eb$ ,  $M(E4) = +0.0070 eb^2$  and  $M(E6) = -0.00008 eb^3$ , with similar errors. This value of  $M(E2)$  is within 1% of that obtained in Ref. 1.

#### IV. OTHER EXCITED STATES

DWBA calculations have been performed for the bulk of the data for  $^{24}\text{Mg}$  as shown by the curves in Figs. 6–17 and for that of  $^{26}\text{Mg}$  shown in Figs. 18–29. The more ambitious CC calculations necessary for some of these data<sup>6,7</sup> are deferred. The parameters of the spherically symmetric optical potential are given in Table I and the deformation parameters are summarized in Tables III and IV. The deformation lengths  $\beta_l R$  are only given for states for which the DWBA results are reasonable fits.

Some general features of the data are apparent. There are a variety of shapes of  $\sigma(\theta)$  for states of the same angular momentum transfer, for example the first three  $4^+$  states of  $^{24}\text{Mg}$ , but  $A_y$  for such states differ only by shifts in the position of the sharp drop and subsequent rise to higher positive values, typically around 0.4. States with rather flat featureless cross sections have constant  $A_y$

values of  $\sim 0.4$  to  $0.6$ . Indeed, nearly all data points are positive. The values of  $A_y$  for proton plus nucleon elastic scattering are also positive with a rise to between 0.3 and 0.5 at 800 MeV.<sup>15</sup> Negative or small values of  $A_y$  seen for  $1^+$  states in  $^{12}\text{C}$  (Ref. 16) are not observed here.  $A_y$  for the  $3^+$  data is consistent with a constant value of 0.6. Thus the data for  $A_y$  are consistent with a two-body operator for the excitation with spin structure much like that for the free proton-nucleon system.

The effective nuclear radius for spin-down cross sections is slightly larger than for spin-up cross sections. This combined with a lower strength for spin down leads to minima at slightly larger angles than that for the spin up and causes  $A_y$  to increase with angle except in the region of minima in spin up where the cross section for spin down is almost equal, causing a minimum in  $A_y$  followed by a rise in  $A_y$  as the spin-down cross section goes into a minimum.

The deformation lengths obtained here for  $^{26}\text{Mg}$  are about 20% lower than those obtained in Ref. 1 with a potential with no spin-orbit contributions. This is despite an increase in the radius of the volume potential over that used in Ref. 1.

TABLE III. Previously observed levels in  $^{24}\text{Mg}$  and those observed in this paper. Also given are parameters used in describing these states with DWBA calculations.

Previously observed (Ref. 8)		Present paper, DWBA			
$E$ (MeV)	$J^\pi$	$E$ (MeV) <sup>a</sup>	$l$ transfer	$\beta_l$	$\beta_l R$ (fm) <sup>b</sup>
1.369	$2^+$	1.37	2	0.67	1.77
4.123	$4^+$	4.12	4	0.077	
4.238	$2^+$	4.24	2	0.163	0.43
5.236	$3^+$	5.24	3		
6.010	$4^+$	6.01	4	0.334	0.88
6.432	$0^+$	6.43	0	0.071	
7.348	$2^+$	7.35	2	0.140	
7.616	$3^-$	7.62	3	0.249	0.66
8.113	$6^+$	8.12	6	0.032	
8.358	$3^-$	8.36	3	0.292	0.77
8.437	$(3,4)^+ + 1^-$	8.44	4	0.127	
8.653	$2^+$	8.65	4	0.025	
9.148	$1^-$	9.15	4	0.057	0.151
9.283	$2^+$	9.28	2	0.071	
9.528±9.52	$6^+ + 4^+, T=1$	9.53	6	0.091	0.24
10.026	$5^-$	10.10	5	0.217	0.57
		10.44			
		10.68	4	0.071	0.186
		11.10	3	0.118	0.311
		11.53	1	0.033	
		11.78	2	0.077	
14.15	$8^+$	14.15			
		14.50			
15.120	$6^-, T=1$	15.20			(15.137) (Ref. 17)
15.436	$0^+, T=2$	15.37			
15.54, 15.64		15.54			

<sup>a</sup>0.0 to 7.62 MeV states from Endt and Van der Leun (Ref. 8) have been used for calibration in the present work.

<sup>b</sup>Deformation length values are given for states where the DWBA curves are a reasonable description of the magnitude of the angular distribution.

A.  $^{24}\text{Mg}$ 

Data for  $2^+$ ,  $3^+$ ,  $4^+$ , and  $6^+$  states, which were considered as members of a  $\gamma$ -vibrational band in Ref. 1, are given in Figs. 6 and 7. The difference in the DWBA curves and the data show that CC calculations (as in Refs. 1, 6, and 7) are necessary to explain the data for the  $2^+$  state, particularly the strength of the second maximum and the position of the first minimum. The slight structure in  $\sigma(\theta)$  for the  $3^+$  is not apparent in  $A_y$ , which is constant at about 0.6. The good fit to the  $4^+$  strength supports the inclusion of a  $Y_{42}$  coupling to the ground state. The first maximum for the  $6^+$  has shifted from  $16^\circ$  for the DWBA to  $13^\circ$ . The CC results from Ref. 1 showed this state to be explained by a dominant two step contribution.

The data shown in Figs. 8 and 9 are for possible members of a monopole band. There is an obvious need for a direct coupling to the ground state similar to that of Ref. 17.

Data for two  $3^-$  and a  $5^-$  state are given in Figs. 10 and 11. The shift in the minima of the  $3^-$  states are due

to  $K$  dependent effects.<sup>1</sup> The shallow minimum in  $\sigma(\theta)$  for the 7.63 MeV state results in a rather smooth variation in  $A_y$ , while the well defined minimum in  $\sigma(\theta)$  for the 8.36 MeV state leads to structure in  $A_y$ . The peak of the  $5^-$  is seen to be shifted to smaller angles than the DWBA result.

Some states with rather strange  $\sigma(\theta)$  are shown in Figs. 12 and 13. The 9.28 data are more consistent with  $l=1$  and some structure is seen in  $A_y$ . The 8.65 could be excited by  $l > 4$ , while the peak at 10.44 MeV seems to be a sum of states of different spins.

The fit of the 10.68 MeV state with  $l=4$  is good as seen in Figs. 14 and 15. The 11.10,  $3^-$  is not as well explained, having a slope less than that for the DWBA calculation. This could indicate multistep excitation. The 11.53 and 11.78 MeV states have rather imaginative "fits" and are difficult to explain.

No fits have been attempted to the data shown in Figs. 16 and 17. All have flat or broad  $\sigma(\theta)$  and flat  $A_y$  of about 0.4. Five points with small  $A_y$ 's are seen for the 14.50 MeV peak. The  $\sigma(\theta)$  values for these points are lower than the neighboring points indicating a problem

TABLE IV. Previously observed levels (Ref. 8) in  $^{26}\text{Mg}$  and those observed in this paper. Also given are parameters used in describing these states with DWBA calculations.

Previously observed (Ref. 8)		Present paper, DWBA			
$E$ (MeV)	$J^\pi$	$E$ (MeV) <sup>a</sup>	$l$ transfer	$\beta_l$	$\beta_l R$ (fm) <sup>b</sup>
1.809	$2^+$	1.81	2	0.44	1.34
2.938	$2^+$	2.94	2	0.142	0.43
3.588	$0^+$	3.59			
3.941	$3^+$	3.88			
4.318	$4^+$	4.33	4	0.10	0.32
4.332	$2^+$	4.33	2	0.064	0.19
4.350	$3^+$				
4.834	$2^+$				
4.900	$4^+$	4.90	4	0.165	0.50
4.972	$0^+$				
5.291	$2^+$	5.29	2	0.086	
5.473	$4^+$	5.47	4	0.092	0.28
5.716	$4^+$	5.72	4	0.095	0.29
6.878	$3^-$	6.88	3	0.162	0.49
6.256	$0^+$	6.26			
6.744	$2^+$	6.74	2	0.025	
7.099	$2^+$	7.10			
7.36 <sup>c</sup>		7.34			
7.69(2), $3^-$ <sup>c</sup>		7.69	3	0.081	0.25
7.83(2), $3^-$ <sup>c</sup>		7.83	3	0.131	0.40
		8.03	6	0.055	0.17
8.19(2), $3^-$ <sup>c</sup>		8.23	3	0.167	0.51
8.53(2), $2^+$ <sup>c</sup>		8.53			
		8.70	4	0.065	0.20
8.89(1), $2^+$ <sup>c</sup>		8.95			
9.29(2), $2^+$ <sup>c</sup>		9.25	4	0.084	0.25
10.33(2), $3^-$ <sup>c</sup>		10.40	4	0.112	0.34

<sup>a</sup>0.0 to 6.88 MeV states from Endt and Van der Leun (Ref. 8) have been used for calibration in the present work.

<sup>b</sup>Deformation length values are given for states where the DWBA curves are a reasonable description of the magnitude of the angular distribution.

<sup>c</sup>Results from (e,e'), E. W. Lees *et al.*, J. Phys. A 7, 936 (1974).

with the extracted spin-up cross section. The 15.2 MeV state is most probably the  $T=1, 6^-$ , 15.137 MeV state of Ref. 18. The spin-flip amplitude is much larger for 100–200 MeV ( $p, p'$ ) excitation than about 800 MeV. The  $6^-$  is much larger than neighboring states at 135 MeV, but is less than or equal to them at 800 MeV. The peak cross section here is  $\sim 0.025$  mb/sr as compared to 0.1 at 135 MeV.<sup>17</sup> The average of  $A_y$  for the  $6^-$  is slightly smaller than other states in the vicinity but not small or negative as for the  $1^+$  states in  $^{12}\text{C}$ .<sup>16</sup>

### B. $^{26}\text{Mg}$

The data for possible members of a  $K^\pi=2^+$  band as assumed in Ref. 1 are given in Figs. 18 and 19. The fit to the  $2^+$  is good until after the second maximum while there is an obvious shift inward for the  $4^+$ . The maximum of  $\sigma(\theta)$  for the  $3^+$  is less than that for  $^{24}\text{Mg}$ , and  $A_y$  is poorly determined. CC calculations are necessary for these data.

A monopole coupling to the ground state<sup>18</sup> is necessary to analyze the data for the (3.59,  $0^+$ ) and (5.29,  $2^+$ ) given in Figs. 20 and 21. The data for the 6.26 MeV state are too sparse for a reasonable analysis while the weakly excited state at 6.7 MeV seems to be at least  $l=4$  or perhaps dominated by two step contributions.

The first four  $4^+$  states are given in Figs. 22 and 23. As discussed earlier the 4.3 is actually a sum of  $2^+$  and  $4^+$  and an incoherent sum has been made of DWBA calculations. The fits are good with some apparent differences in the first minimum. The analyzing power calculations are systematically lower than the data in the region of the first maximum for  $\sigma(\theta)$ , indicating a general failure of the calculations since this is independent of  $\beta_4$  and most coupled channels effects.

Data for the four  $3^-$  states are given in Figs. 24 and 25.  $K$  dependent effects<sup>1</sup> are obvious in the shifts inward and outward for the 7.83 and 8.23 MeV states, respectively, while the DWBA is correct for the 6.88,  $3^-$ . These three states are excited with comparable strength and the  $A_y$  values are explained except for position of the structure. The 7.69 MeV state is much weaker and is probably the sum of a  $3^-$  with an even multipole, producing a smoothly falling  $\sigma(\theta)$  and flat  $A_y$ .

Data for four states with  $\sigma(\theta)$  similar to that for  $l=2$  are shown in Figs. 26 and 27. The success of the DWBA in explaining  $A_y$  for the first three supports the  $l=2$  assumption. However, more complex calculations are necessary to explain the strength and shape of  $\sigma(\theta)$ . The 8.95 MeV state is probably the sum of different levels with different multipoles.

Finally in Figs. 28 and 29 are data for three additional

$4^+$  states in  $^{26}\text{Mg}$ . The shifts in the first two are reflected by flat  $A_y$  values while the stronger 10.4 MeV state has an  $A_y$  with clear structure indicative of  $l=4$ . As for the first four  $4^+$  states, the data for  $A_y$  is higher than the DWBA values in the region of the first maximum in  $\sigma(\theta)$ . The lower value of  $\beta_4$  utilized here for the 10.4 state results from requiring that the DWBA results not be above the data in the region of the first maximum.

## V. SUMMARY AND CONCLUSIONS

Angular distributions and analyzing power data have been presented above for polarized proton scattering from  $^{24}\text{Mg}$  and  $^{26}\text{Mg}$  at 0.8 GeV for 26 excited “states” in  $^{24}\text{Mg}$  and 23 excited “states” in  $^{26}\text{Mg}$ . Although there are a variety of shapes for the angular distributions, the analyzing power data for all states are positive and similar in magnitude, and seem to be consistent with a two-body operator for the excitation with a spin structure much like that for the free proton-nucleon system.

Evidence for a level at 8.03 MeV with  $J > 4$  in  $^{26}\text{Mg}$  has been presented. The position of the first maximum of the angular distribution (characteristic of  $l=5$  or 6), the results of the coupled channels and DWBA calculations, the observed trend of the angular distributions of excited states in neighboring nuclei, and rigid rotor predictions all yield support for this conclusion, and suggest most probably that  $J^\pi=6^+$ .

Coupled channels analyses of the data for the excitation of the  $0^+$ ,  $2^+$ ,  $4^+$ , and  $6^+$  members of the ground state rotational band in  $^{24}\text{Mg}$  and  $^{26}\text{Mg}$  describe the data reasonably well. When combined with the known charge moments, the moments of the deformed optical potential obtained in the present analysis imply that the moments of the neutron and proton distributions in  $^{26}\text{Mg}$  are approximately equal and prolate and that the signs of the  $M(E4)$  and  $M(E6)$  are negative.

Distorted wave Born approximation calculations have been compared with the bulk of the data. More complex coupled channels calculations are needed to explain the complicated vibrational bands built upon the ground state rotational band.

## ACKNOWLEDGMENTS

This research was supported in part by the U.S. National Science Foundation, the U.S. Department of Energy, and the Robert A. Welch Foundation.

\*Present address: Arizona State University, Tempe, Arizona 85287.

†Present address: Los Alamos National Laboratory, Los Alamos, New Mexico 87545.

‡Present address: CEBAF, Newport News, VA 23606.

§Present address: Institut des Sciences Nucléaires, Grenoble,

France.

<sup>1</sup>G. S. Blanpied *et al.*, Phys. Rev. C **25**, 422 (1982), and references contained therein.

<sup>2</sup>G. S. Blanpied *et al.*, Phys. Rev. C **30**, 1233 (1984).

<sup>3</sup>D. K. Hasell, Phys. Rev. C **27**, 482 (1983).

<sup>4</sup>F. Sciuccati, S. Micheletti, M. Pignanelli, and R. DeLeo, Phys.

- Rev. C **31**, 736 (1985).
- <sup>5</sup>R. de Swinarski, F. G. Resmini, D. L. Hendrie, and A. D. Bacher, Nucl. Phys. **A261**, 111 (1976).
- <sup>6</sup>P. W. F. Alons, H. P. Blok, J. F. A. Van Hienen, and J. Blok, Nucl. Phys. **A367**, 41 (1981).
- <sup>7</sup>B. Zwiaglinski, G. M. Crawley, J. A. Nolen, Jr., and R. M. Ronningen, Phys. Rev. C **28**, 542 (1983).
- <sup>8</sup>P. M. Endt and C. Van der Leun, Nucl. Phys. **A310**, 1 (1978).
- <sup>9</sup>S. Kubono *et al.*, Phys. Lett. **103B**, 320 (1981).
- <sup>10</sup>G. W. Hoffmann *et al.*, Phys. Rev. C **24**, 541 (1981).
- <sup>11</sup>See AIP Document No. PAPS PRVCA 37-1987-191 for 191 pages of numerical data for 0.8 GeV scattering of polarized protons from <sup>24,26</sup>Mg. Order by PAPS number and journal reference from American Institute of Physics. The price is \$3.00 for microfiche or \$29.15 for photocopies airmail extra.
- <sup>12</sup>J. Raynal, International Atomic Energy Agency Report IAEA-SMR-918, 1972 (unpublished).
- <sup>13</sup>W. Chung, Ph.D. thesis, Michigan State University, 1976 (unpublished).
- <sup>14</sup>R. H. Spear, T. H. Zabel, M. T. Esat, A. M. Baxter, and S. Hinds, Nucl. Phys. **A378**, 559 (1982).
- <sup>15</sup>M. L. Barlett *et al.*, Phys. Rev. C **27**, 682 (1983).
- <sup>16</sup>K. Jones, Ph.D. thesis, Rutgers University, 1982 (unpublished).
- <sup>17</sup>G. S. Adams *et al.*, Phys. Rev. Lett. **38**, 1387 (1977).
- <sup>18</sup>M. N. Harakeh and R. DeLeo, Phys. Lett. **117B**, 377 (1982).